Corresponding Author:

Jonathan Farley

Ricardo Plc

Southam Road

Radford

Leamington Spa

CV31 1FQ

07787872886

Jonathan.farley@ricardo.com

Low Cycle Fatigue Simulation and Fatigue Life Prediction of Multilayer Coated Surfaces

Jonathan Farley[1], Luiz C. Wrobel[2], Ken Mao[3]
[1]Ricardo Plc, Southam Road, Radford, Leamington Spa, CV31 1FQ
[2]School of Engineering & Design, Brunel University, Uxbridge, UB8 3PH
[3] School of Engineering, University of Warwick, Coventry, CV4 7AL

ABSTRACT

This paper focuses on the simulation of low cycle fatigue (LCF) failures in highly loaded coated surfaces subjected to mixed rolling-sliding contact in dry conditions. The development of an advanced finite element (FE) model and creation of a unique user-defined subroutine are used to predict subsurface crack initiation in multilayer surfaces. Through the application of shakedown principles and the critical crack plane theory the developed subroutine, running concurrently with the FE solver, is used to predict the location and orientation of the LCF initiation point for a Tungsten Carbon-Carbide (WC-C) coated surface.

Furthermore, a detailed physical wear study is presented from tests on a number of WC-C coated samples subjected to dry mixed rolling-sliding contact under high load. Images of the progressive breakdown of the coated surface are presented along with a detailed discussion of the coating failure mechanisms. Comparison of the results from the simulation and physical tests are made and conclusions drawn.

KEYWORDS

Low Cycle Fatigue, Fatigue Life Prediction, Surface Coating, FEA, Shakedown, Critical Crack Plane

INTRODUCTION

The effects of cyclic loading, particularly in the region of plastic material response, can be very detrimental to the fatigue life of a component. The rate at which a material will fail under fatigue has been linked to a number of factors such as stress, strain, temperature changes and corrosion [1]. For low cycle fatigue failures, the damage associated with the

accumulation of plastic strains has been found to dominate material failure. Although the application of surface coatings may go some way to reducing the loads experienced by the substrate, in cases of very high loading, significant plastic deformation of the subsurface material may still occur.

In this paper, an advanced finite element analysis software (Abaqus) is extended to offer a simple tool for fatigue life calculation of multilayer coating systems. The development of a fatigue life prediction routine coupled to the Abaqus solver provides a means of generating simulation results which are then used to calculate the material fatigue life. In this study, this method is applied to predict the fatigue life of simple coated discs subjected to rolling contact fatigue under dry heavy loaded conditions.

In an attempt to verify the simulation results, a number of physical fatigue tests were also conducted on coated test samples to establish a detailed understanding of the progressive wear and surface failure evident from the application of heavy cyclic mixed rolling-sliding loading. The results from the physical tests are compared and contrasted with the results from the simulations and some conclusions made.

Low Cycle Fatigue and Shakedown

Low Cycle Fatigue (LCF) refers to the failure of a material loaded in the region of plastic material response as a result of repeated loading. This response is highly variable and much harder to predict than more traditional High Cycle Fatigue (HCF) failures. LCF failures typically occur in the order of a few thousand load cycles rather than the million cycles expected for HCF. Research into new methods of LCF prediction has begun to focus around the application of shakedown principles [2, 3].

Shakedown principles were developed in the mid 1900s to assist with the analysis of elastic-plastic materials subjected to repeated loads, and were shown to have significant advantages over previously used methods. Firstly, they concentrate on the cyclic state of the material directly, negating the need to determine the plastic loading history of the material from the

beginning. Secondly, they are driven by the elastic stress distribution in the material rather than the elastic-plastic material stresses which are comparatively much harder to obtain. As a result, shakedown principles offer a more accessible method for determining a material's response to cyclic loading.

Materials subjected to repeated loads show four types of material response; (a) Perfectly elastic response, (b) Elastic shakedown (c) Plastic shakedown and (d) Ratchetting (Figure 1).

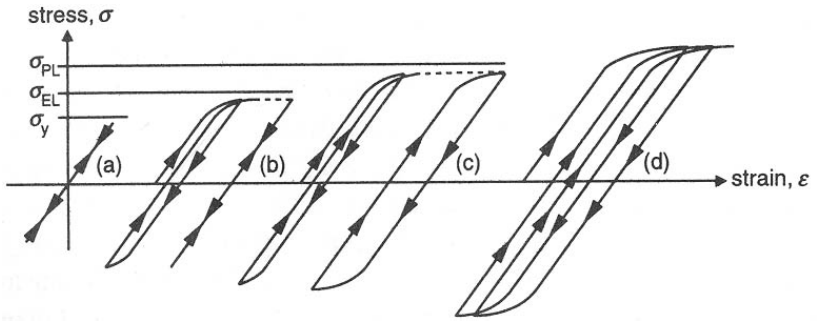

Figure 1 – Material Response Diagram [2]

Shakedown theory is concerned with determining the conditions (loading, temperature, contact conditions, etc) at which a material will transfer between these four types of material response. Through detailed investigation, Melan [4], Koiter [5] and Ponter [6] identified that the variation of the shakedown limit of a material is predominantly governed by three criteria: residual stress, strain hardening and geometry changes as a result of plastic deformation.

Although shakedown describes the general response of a heavily loaded surface relating the interfacial friction with the applied load, shakedown principles do not directly outline the workable life of a loaded surface or the resulting failure mechanism. For this reason, a more detailed method of determining the subsurface stress and strain states is required. To provide this, shakedown principles have been combined with the critical crack plane theory.

Critical Crack Plane Theory

The effect of cyclic loading induced from rolling contact conditions on the surface of a component causes a non-proportional cycle of tension, shear and compression in the

underlying subsurface material and an effective tensor rotation of stresses and strains. As a result, large magnitudes of strain and shear may exist from the combined effect of each individual component at any angle within the material. This plane is termed the critical crack plane (Figure 2) and can be determined through a tensor rotation of the principal strains calculated from a finite element model.

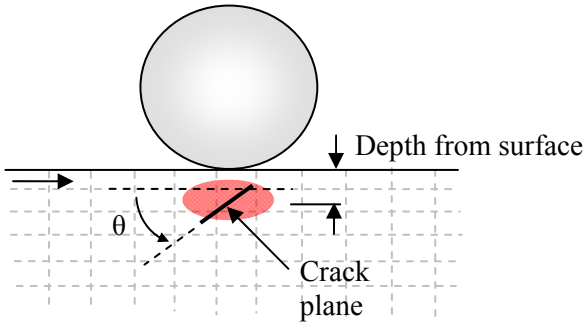

Figure 2 – Definition of location and orientation of the critical crack plane

The aim of this investigation is to improve the understanding of how subsurface crack initiation may be affected by the application of coatings to surfaces that are loaded near or above the material plastic response region. An adapted Coffin-Manson equation presented by Bannantine et al. [7] has been used as the fatigue check criteria in this study. This equation provides consideration for both the high shear strain characteristics present during crack initiation and for fatigue life calculations where material strain, rather than stress, dominates the fatigue life, and has the form:

$$\frac{\Delta\gamma}{2} = \frac{\tau_f'}{G}(2N_f)^b + \gamma_f'(2N_f)^c \qquad (1)$$

where:

$\Delta\gamma$ = Change in shear strain

τ'_f = Shear fatigue strength coefficient

γ'_f = Shear fatigue ductility coefficient

G = Shear elastic modulus (Pa)

b = Fatigue strength exponent

c = Fatigue ductility exponent

N_f = Fatigue life (cycles)

1. LOW CYCLE FATIGUE SIMULATION OF COATED SURFACES

To investigate the potential benefits of the application of a tribologically advanced coating to the surface of a component subjected to cyclic loading, a simple multilayer contact model was developed to simulate contact of multiple step or repeated loading conditions. Through the application of shakedown principles and fatigue crack initiation criteria, detailed material information calculated during the simulation is then used to estimate the fatigue life of the model.

Simulation of Fatigue in Tungsten-Carbon Carbide

The model developed in this study was based on the initial model developed by Farley et al. [8] to investigate thin film surface coatings. The model was applied to simulate the response of a very thin multilayer low friction Tungsten Carbon-Carbide (WC-C) coating currently being used in a number of automotive applications. The coating consists of a 1μm WC-C layer dense in anamorphous carbon particles bonded with tungsten. This is built on a 0.2μm Chromium interlayer applied as an adhesive aid to the substrate. The substrate used in the simulation was a Chromium-Molybdenum steel with a hardness of 58HrC. The full details of the material properties are given in Table 1. The model, replicating a twin-disc contact test, simulates a small segment of each disc One of the discs represents the test sample and consists of the substrate with coating layers, modelled as fully deformable. The other represents the driving disc and is modelled as a rigid indenter as shown in Figure 3. A constant vertical load is applied to the rigid indenter to establish the required contact pressure between the disc sections. Next, a fixed angular rotation was applied to each disc, through non-zero boundary constraints, to introduce the required relative motion (or slip) into the contact. A pattern of cyclic loading is established by simply returning the model to the start

position under zero contact load and reapplying the load and slip. This simple method of step duplication, although computationally demanding, can be used to generate a detailed loading history as the simulation progresses, providing essential information required for fatigue life prediction.

Table 1 – Simulation properties used for the LCF model

Material	Coating layer	Thickness t (μm)	Young's Modulus E (GPa)	Poisson's Ratio	Hardness (HV)	Friction (μ)
Substrate	-	-	209	0.29	748	0.4*
Coating	WC/C	1.00	250	0.25	1050	0.1*
	Cr	0.20	140	0.22	800	

* Dry, against steel

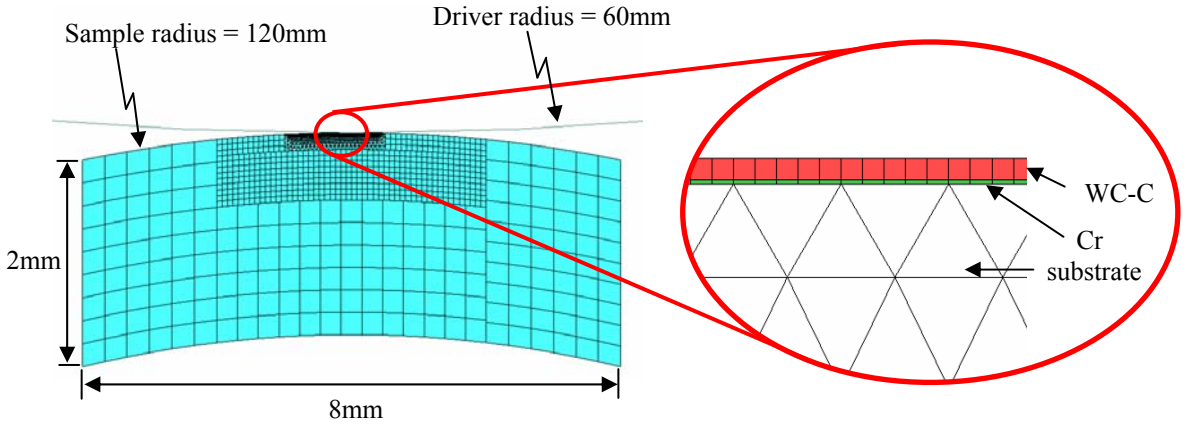

Figure 3 – Mesh definition for coated shakedown model

Coffin-Manson LCF User-Defined Subroutine

Abaqus user-defined subroutines allow the addition of further simulation capabilities to the standard Abaqus solver. Operating concurrently with the solver, user-defined subroutines can be executed during the analysis to modify various characteristics whilst the simulation progresses. Using this capability, a FORTRAN routine was developed to obtain details of the

material loading. These are then applied to the Coffin-Manson equation to calculate the material fatigue life.

Figure 4 presents a simple flow diagram of the subroutine and the fatigue life calculation procedure developed. The routine retrieves the strain data from each of the mesh integration points in the FE model at every load step increment. Tensor rotations are performed to detect the maximum strain amplitude in the material and search for the critical crack plane. This amplitude and its orientation are recorded and the solver progresses to the next step. The result is a 'map' of the shear strain range history across the entire substrate, which is then applied to the Coffin-Manson shear strain fatigue life equation (Eq 1) to determine the material fatigue life, and the location and orientation at which it occurs.

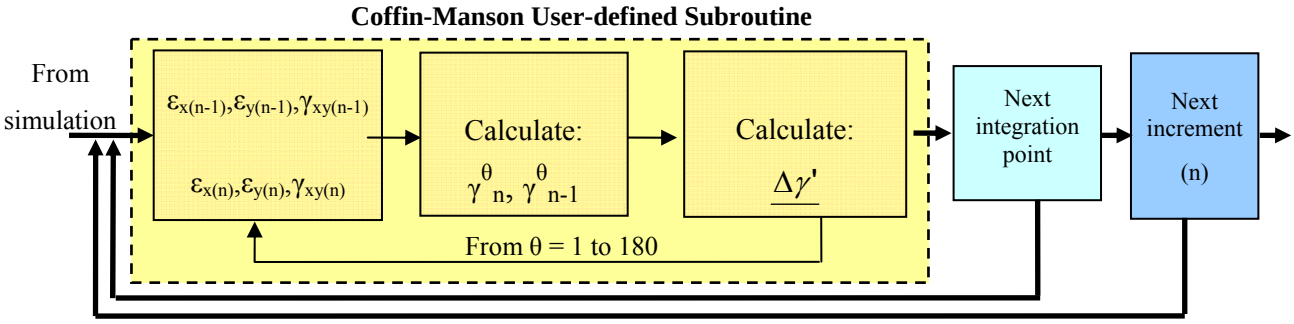

Figure 4 – Coffin-Manson user-defined subroutine procedure

This method is very efficient when compared to typical post-processing approaches. With this method, the subroutine runs concurrently with the simulation, processing the fatigue data in 'real time', allowing the simultaneous calculation of various fatigue criteria. The results from the subroutine can also be used to control the simulation, stopping the simulation when a 'target' value is achieved or driving adaptive mesh functionality to enhance the mesh quality in areas with the highest shear strains.

To investigate the variation of fatigue life achieved through the addition of a WC-C coating to the surface of the substrate, six different low cycle fatigue simulations were conducted. A shakedown map presented by Johnson [9] for mixed rolling-sliding contact was used to identify the contact pressures required to obtain the substrate material response of interest can

be identified in Figure 5. The diagram offers a quick estimation of the material response in relation to non-dimensional factors P_0/K (maximum Hertzian contact pressure / shear yield stress) and μ (traction or friction coefficient).

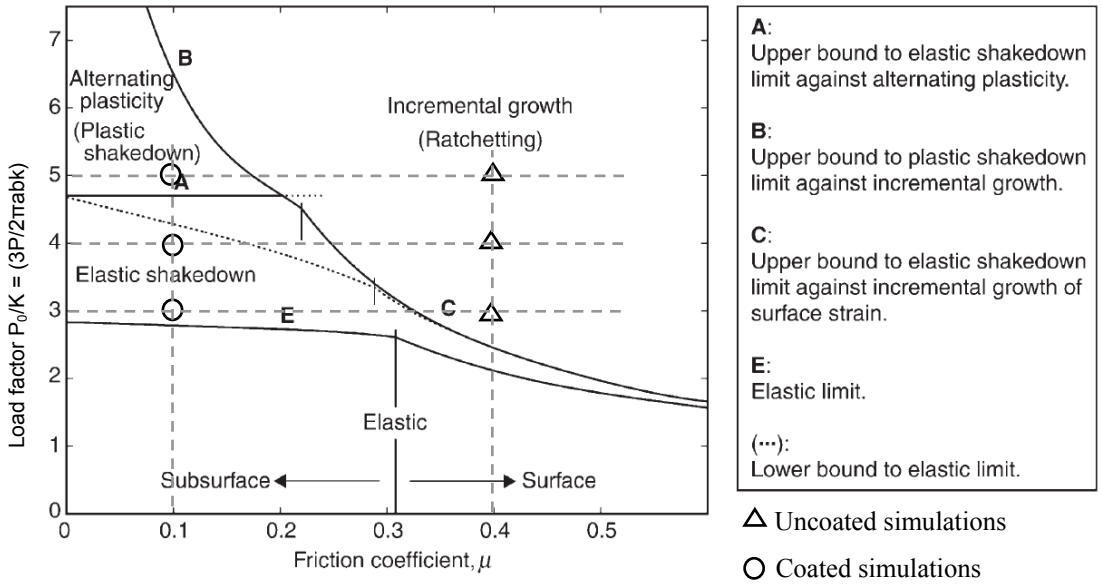

Figure 5 – Two-dimensional shakedown map identifying the predicted response for the simulations [9]

Coating Simulation Results

Using the fatigue subroutine to conduct a search for the location of maximum strain accumulation, a plot of the component of the substrate stress and strain values acting radically from the contact centre is presented for each simulated load case, Figures 6 and 7. For the uncoated model simulation, a classic pattern of plastic shakedown and incremental ratchetting is observed. With the lower load case of $P_0/K = 3$, initial plastic deformation occurs before the material shakes down to a closed loop of plastic deformation. For the higher load cases, $P_0/K = 4$ and $P_0/K = 5$, a more distinct pattern of ratchetting occurs, with small but incremental increases in net strain with every load cycle. This is typical of low level ratchetting growth, the response expected from the shakedown map.

For the coated simulations, the addition of the low friction coating can be seen to reduce the subsurface loading moving the substrate response from a ratchetting response to plastic and

then elastic shakedown. In the first load case, $P_0/K = 3$, elastic shakedown occurs immediately with a highly repeatable cycle of near zero net plastic displacement occurring during every load pass. As the load increases to $P_0/K = 4$, the effects of strain hardening and residual stresses soon result in the stabilisation of the substrate material to a state of plastic shakedown. With the final load case, $P_0/K = 5$, continuous yielding is present within the substrate with small but consistent increases in strain observed with every load pass. However, the fluctuations in strain are distinctly lower than those experienced by the uncoated substrate, suggesting an improvement in substrate durability would be expected as the exhaustive effect on the material ductility is greatly reduced.

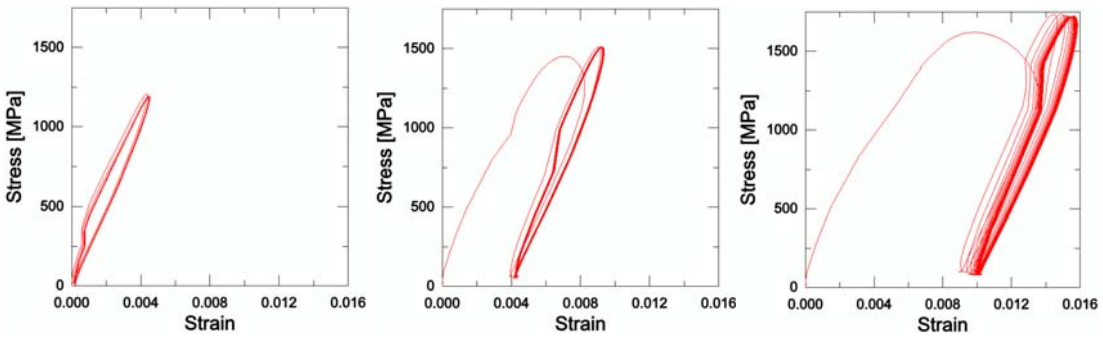

Figure 6 – Radial stress-strain plots at location of maximum shear-strain – Uncoated: $P_0/K = 3$, $P_0/K = 4$, $P_0/K = 5$

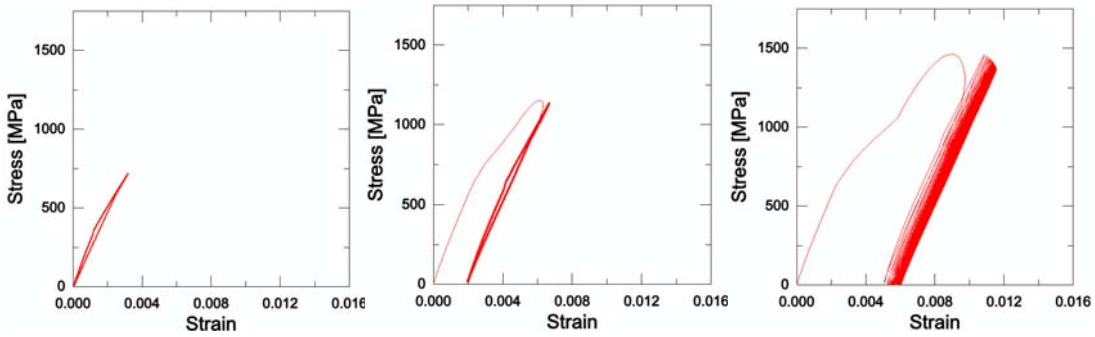

Figure 7 – Radial stress-strain plots at location of maximum shear-strain – Coated: $P_0/K = 3$, $P_0/K = 4$, $P_0/K = 5$

In addition to monitoring the stress and strain states, the Coffin-Manson user-defined subroutine was used to predict the fatigue life of the model. Figure 8 shows a contour plot from the critical crack plane search routine at $P_0/K=5$ for both coated and uncoated

simulations. The difference in the location and magnitude of the maximum shear strain range between the simulations is quite clear. The routine applied here uses the largest shear strain range as the driver for fatigue life, and its location can therefore be considered as the point at which cracks will first occur. The shear strain range plots show that for the uncoated model the maximum shear strain values occur at the contact surface, suggesting crack initiation will occur in the contact zone. This would most likely be visible through the creation of surface pitting, a common cause of component fatigue failures loaded in this way [10]. The results from the coated model simulations show a very different result with the location of the maximum shear strain range well into the substrate, indicating the probable location of crack initiation to be well below the sample surface.

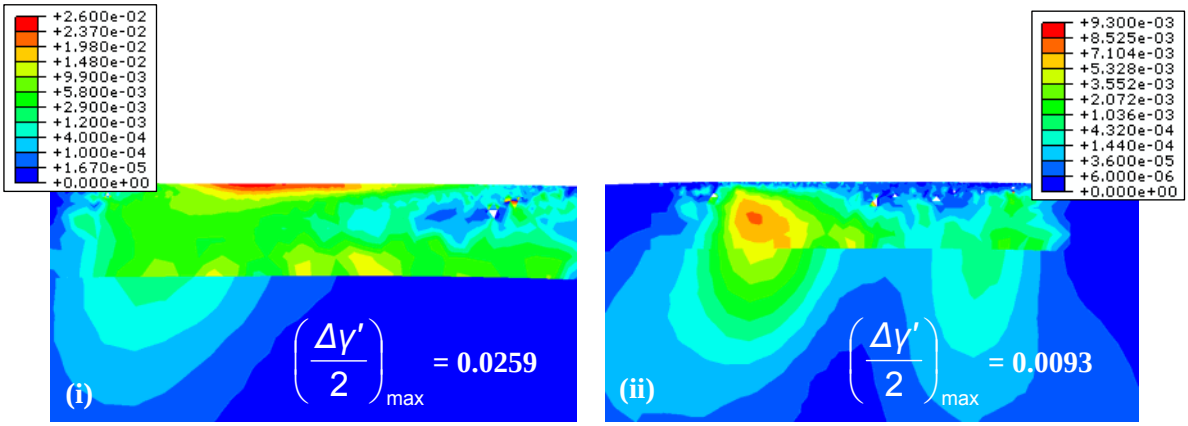

Figure 8 – Contour plots of the maximum shear strain range following 50 cycles at $P_0/K = 5$

(i) Uncoated, (ii) Coated

A full breakdown of the locations of the critical crack plane and estimated fatigue life for each of the simulated load cases is presented in Table 3. It is clear that, for the uncoated model simulations, the maximum shear strain range occurs directly at the contact surface, parallel to the interface. The estimated fatigue life proved to be outside the predicable range of the Coffin-Manson method used, showing zero fatigue life for simulations above $P_0/K = 3$. This would suggest that high levels of subsurface plastic response should be evident right from the first few loading cycles.

For each of the coated simulations, the location of the crack plane was found to be approximately in the order of 0.1mm below the surface, the depth increasing slightly with applied load. For $P_0/K=3$ and $P_0/K=4$, the crack plane was calculated to occur at about $\theta = 13^\circ$ (measured clockwise) from the contact surface. As the load is increased, the angle appears to reduce to $\theta = 2^\circ$, suggesting that with the higher loads, horizontal subsurface cracks should be present within the substrate subsurface region. The addition of the coating also has a significant effect on the calculated fatigue life. When directly compared to the uncoated simulations, the fatigue life is orders of magnitude higher. This is due to the reduced subsurface stresses and reduced shear strain range, equating to a greatly increased fatigue life.

Table 3 – Fatigue life and Critical Crack Plane location and orientation results

Model simulation	P_0/K	Max Shear Strain amplitude $\left(\frac{\Delta\gamma'}{2}\right)_{max}$	Predicted Fatigue life (cycles)	Critical Crack Plane	
				Depth from surface (mm)	Angle (degs)
Uncoated	3.0	0.0145	1524	Contact zone	0
	4.0	0.0220	0	Contact zone	0
	5.0	0.0259	0	Contact zone	0
Coated	3.0	0.0023	549974	0.121	13.5
	4.0	0.0045	41270	0.155	12.8
	5.0	0.0093	4855	0.154	1.8

2. LOW CYCLE FATIGUE TESTS OF COATED SURFACES

In order to test the LCF properties of the simulated coating, a number of twin disc tests were conducted with coated test samples. The testing equipment used during this investigation is a bespoke test rig designed and manufactured at Brunel University, developed by Farley et al. [8] for RCF tests in coated disc samples. An area of particular interest was to test the coating response under elastic shakedown conditions. To induce this, tests were run at a load of P_0/K

= 3 (equivalent to Hertzian contact pressure of ~2GPa) in dry conditions and with a roll-slide ratio of 10%, replicating the conditions used in the simulation.

Figure 9 presents a number of optical pictures of the test sample surfaces at various intervals during the LCF testing. From simple optical inspection, the progressive wear of the sample surfaces can be clearly seen. Where relatively short run times are used, the sample surfaces show very little evidence of wear. Very little change can be seen between the condition of the sample surfaces after as many as 50,000 revolutions. Close observation of the samples identifies small spots of coating debris (most likely graphite) are apparent attached to the sample surfaces. This is caused by the initial surface wearing of the high carbon coating; however, this appears to be the only visible sign of any surface wearing. From 60,000 cycles, the sample surface shows some signs of initial coating breakdown. This continues at an accelerated rate until at 135,000 cycles, significant proportions of the substrate are now exposed. By 250,000 cycles the substrate surface is completely exposed. The result is a rapid increase in wear rate, higher contact temperatures and greater surface roughness through the development of surface pits and other fatigue-related surface damage.

Figure 10 presents a plot of the measured weight loss from each of the test samples across the range of run times along with a best fit curve and ±30% variation bands. By combining the results obtained from the measured sample weight loss and the detailed surface observations of the test samples, some conclusions about the point of coating failure can be made. Through observation of the samples surfaces shown in Figure 9, there appears to be a marked increase in surface damage when comparing the 75,000 and 135,000 cycle test samples. Although no conclusive failure point appears obvious through the measurement of the sample mass loss as presented in Figure 10, there does appear to be a significant increase in sample mass loss at approximately 100,000 – 125,000 cycles. Based on the results of the recorded mass loss and the observations of the samples surfaces, it has been determined therefore that the protective benefits of the high carbon coating appear significantly diminished after 100,000 load cycles or more.

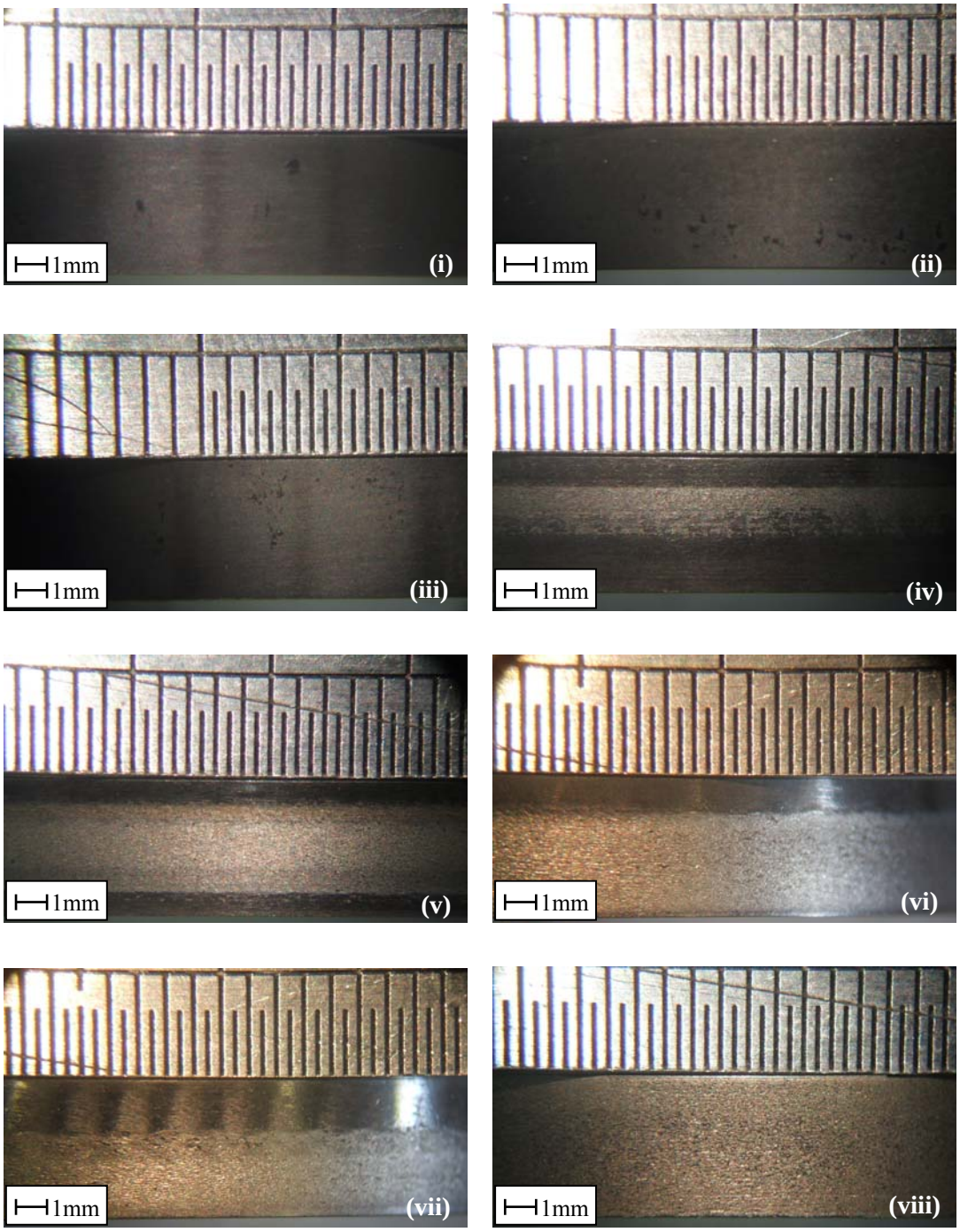

Figure 9 – Optical inspection of the coated test samples surfaces after 2GPa LCF testing (i) 30,000cyc (ii) 40,000cyc, (iii) 50,000cyc (iv) 60,000cyc, (v) 75,000cyc (vi) 135,000cyc, (vii) 190,000cyc (viii) 250,000cyc

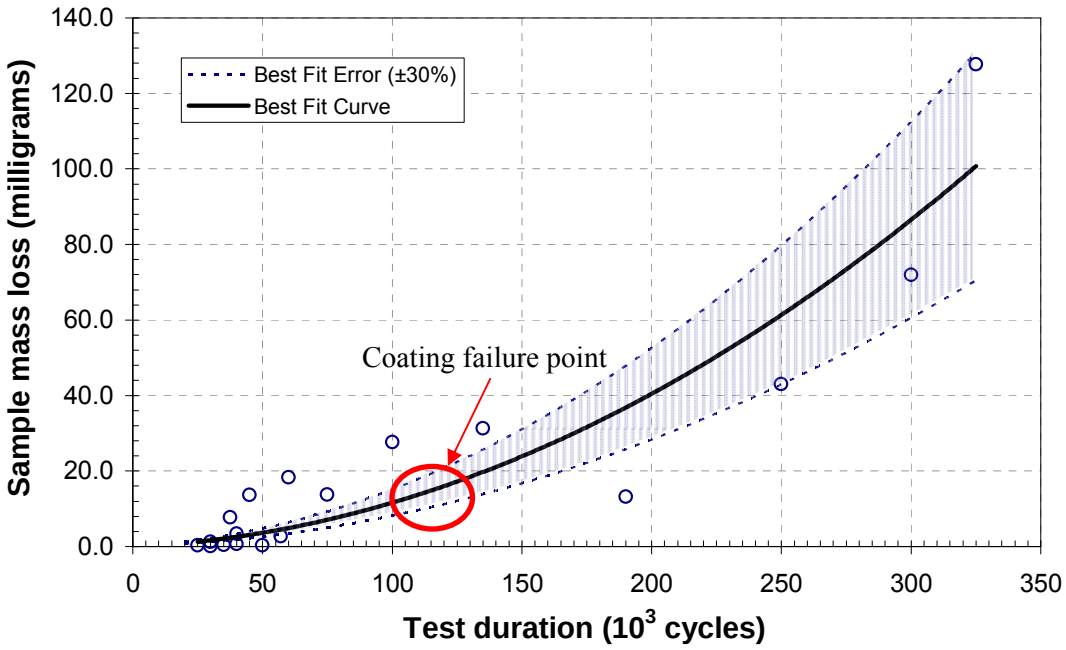

Figure 10 – Coated sample measured weight loss over the range of run times tested

To investigate the condition of the subsurface and help identify the failure mechanisms, Scanning Electron Microscope (SEM) was used to inspect a number of sample cross sections. Figure 11 shows some SEM images of the cross-section from a test sample following a 30,000 cycle test. X-Ray backscatter techniques were used to identify the various material elements and highlight the transition between the substrate, interlayer and coating. The large particles of chromium (bright) and vanadium (dark) are clearly visible in the composition of the steel. The chromium interlayer can be identified as the thin bright layer, its undulations caused by asperities in the substrate. The final top layer, the tungsten carbon-carbide layer (grey), is also visible; however, it can be observed to be much smoother, indicating that large asperities have been removed from the coating surface through 'running in', smoothing the contact surface and reducing the stress through the resulting increase in contact area.

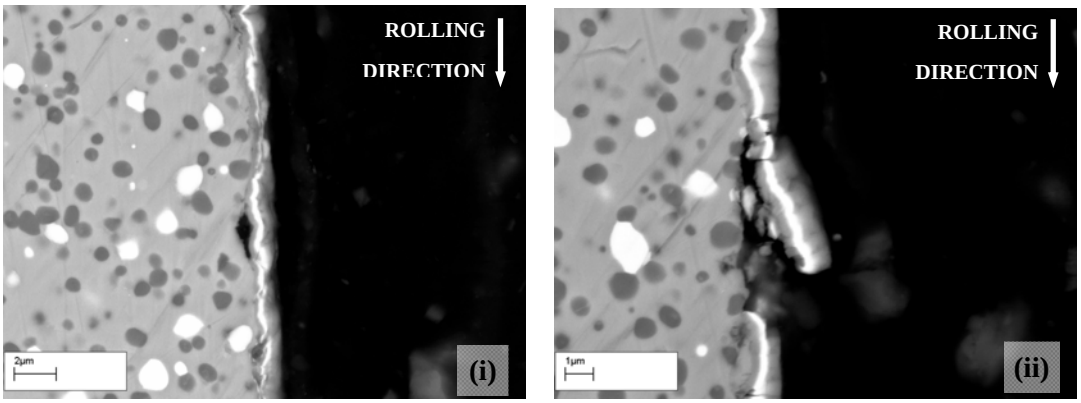

Figure 11 – SEM X-Ray backscatter of WC-C coating, cross section after 30,000 cycles

(i) Subsurface crack growth (ii) Failure of coating

Close inspection of the coating-substrate transition also identifies a number of subsurface cracks appearing just below the chromium interlayer, as can be seen in Figure 12(i). These cracks appear to emerge parallel to the contact surface at about 0.5µm below the substrate-interlayer transition. Prior to coating, the substrate samples were finish ground to 0.4Ra; however, it is clear that a number of residual machining marks are still visible in the substrate surface. The depth of these grooves is significantly larger than the thickness of the 0.2µm chromium interlayer. As a result, when applied to the surface, the chromium layer fills the recesses resulting in a build up of material penetrating the substrate surface. As the contact load passes over the coated surface deformation occurs, creating high stress concentrations in the chromium layer. Over a number of load passes, this stress and strain concentration appears to exhaust the ductility of the substrate material, resulting in crack initiation and eventually subsurface crack growth. Through cyclic loading the crack eventually reaches a critical length, causing propagation to the surface and complete removal of the coating as can be seen from Figure 12(ii).

A direct comparison of the results from the physical tests and the simulation shows something of a different nature. From the calculations performed using the Coffin-Manson subroutine, the fatigue life prediction for the contact model was approximately 500,000 cycles. The simulations also predicted the critical crack plane to be approximately 500µm from surface.

This differs from the results of the physical tests, which suggest coating failure occurs at approximately 100,000 cycles and with cracks starting 0.5-1μm from the surface. One of the main reasons for the differing results stems from the fact that the simulation model does not consider surface irregularities and interlayer stress concentrations. Since the coating was determined to have failed through stress concentrations in the Chromium interlayer promoted by the surface finish defects, the simulation did not account for this. Similarly, the simulations were conducted with ideally smooth surfaces whereas the physical tests were not. The fatigue prediction algorithm was found to be very sensitive to input values so these factors alone may account for the life prediction differences.

CONCLUSION

The first aim of this study was to develop a method for simulating cyclic loading in coating surfaces. The method presented in this paper has been shown to accurately monitor subsurface response and provide close correlation to expected LCF states under specific loading conditions. The method presented is very versatile allowing the simulation of complex geometries and complex loading sequences. Coupled with the user-defined subroutine, the approach outlined here shows the potential to simultaneously calculate fatigue life criteria during the solver, negating the need for extensive post-processing. The multilayer contact model developed in this paper has been shown to clearly identify the potential benefits that can be obtained through the application of advanced surface coatings. Through accurate modelling of material shakedown and the application of the combined Coffin-Manson and Critical Crack Plane methods, both the location and orientation of the point of crack initiation have be identified and the resulting fatigue life calculated.

The second aim of the study was to investigate the protective benefit of the applied coating through physical testing. Using twin-disc tests, a detailed study into the failure rate of a number of coated samples was conducted and used to aid understanding of the coating failure mechanism. Through detailed optical inspection and SEM, coating failure was observed to be caused from subsurface crack initiation just below the surface of the chromium interlayer. A

build up of chromium in recesses remaining in the substrate following surface finishing caused stress concentrations in the substrate material, promoting crack initiation just below the interface. Over progressive loading cycles, these small cracks were seen to propagate, resulting in complete removal of sections of the applied coating and exposing the underlying substrate.

Finally, a direct comparison of the fatigue life prediction results from the tests and simulation were made. This study showed significant differences between the two results caused by a number of factors including modelling simplification, sample surface condition and material properties. Although this investigation goes some way towards providing a simulation method for coated surfaces subjected to complex loading, there is still significant work to be done before life prediction under these conditions can be made with a high degree of accuracy.

ACKNOWLEDGEMENTS

The work described in this paper was supported by the EPSRC. The authors would also like to thank the following companies for their assistance with various parts of this research: Oerlikon Balzers Coatings Ltd, Uddeholm & Abaqus Inc.

REFERENCES

[1] G.E. Dieter, G.E., Mechanical Metallurgy, McGraw-Hill, 1988.

[2] J. Ringsberg, Cyclic ratchetting and failure of a pearlitic rail steel, Fatigue & Fracture of Engineering Materials & Structures 23 (2000) 747-758.

[3] W.R. Tyfour, J.H. Beynon, A. Kapoor, Deterioration of rolling contact fatigue life in pearlitic rail steel due to dry-wet rolling-sliding line contact, Wear 197 (1996) 255-265.

[4] E. Melan, E., Sitzungberichte der Ak., Wien Series 2A 147 (1939) 73-80

[5] W.T. Koiter, A new general theorem on shakedown of elastic-plastic structures. Koninkl. Ned. Ak. Wetenschap B59 (1956).

[6] A.R.S. Ponter, A general shakedown theorem for inelastic materials. Proc. 3rd International Conference on Structural Mechanics in Reactor Technology, Section L, Imperial College, London (1976) 292.

[7] J.A. Bannantine, J.J. Comer, J.L. Handrock, Fundamentals of Metal Fatigue Analysis, Prentice Hall, 1990.

[8] J. Farley, L.C. Wrobel, K Mao, Performance evaluation of multilayer thin film coatings under mixed rolling-sliding dry contact conditions, Wear 268 (2010) 269–276.

[9] A.R.S. Ponter, A.D. Hearle, K.L. Johnson, Application of the kinematical shakedown theorem to rolling and sliding point contacts, Journal of the Mechanics and Physics of Solids 33 (1985) 339–362.

[10] Y. Ding, N.F. Rieger, Spalling formation mechanism for gears, Wear 254 (2003) 1307-1317.